Sources of the oxygen isotopic anomaly in atmospheric N_2O

Mao-Chang Liang[1,2] and Yuk L. Yung[2]

Received 2 August 2006; revised 26 February 2007; accepted 14 March 2007; published 7 July 2007.

[1] One-dimensional and two-dimensional models are used to investigate the isotopic composition of atmospheric N_2O. The sources of N_2O in the atmosphere are based on recent laboratory measurements of the N_2O quantum yield in the mixture of $O_3/O_2/N_2$ (Estupiñán et al., 2002). Two recently proposed pathways (Estupiñán et al., 2002; Prasad, 2005) are evaluated in the model. We find that the new atmospheric sources constitute a few percent of the total N_2O source, but can account for ~50–100% of the $\Delta^{17}O$ anomaly observed in N_2O. The essence of the mechanism is to transfer a heavy oxygen atom originally in O_3 to N_2O. The magnitude of $\Delta^{17}O$ in N_2O is a linear function of the strength of these new N_2O sources. Laboratory and atmospheric measurements are proposed to confirm the chemical pathways. The potential of $\Delta^{17}O$ in N_2O for providing a new tool to probe ozone levels in paleoatmospheres is discussed.

Citation: Liang, M-L., and Y. L. Yung (2007), Sources of the oxygen isotopic anomaly in atmospheric N_2O, *J. Geophys. Res.*, *112*, D13307, doi:10.1029/2006JD007876.

1. Introduction

[2] Nitrous oxide is a potent greenhouse molecule as well as the major source of stratospheric NO_x, which catalyzes the loss of ozone in the stratosphere. The primary sources of N_2O are anthropogenic and oceanic microbial activity as a by-product of nitrification and denitrification reactions, and the major sink is in the stratosphere by UV photolysis [see, e.g., review by *Stein and Yung*, 2003]. The recent discovery [*Cliff and Thiemens*, 1997; *Cliff et al.*, 1999; *Röckmann et al.*, 2001] of an oxygen isotope anomaly in atmospheric N_2O suggests a gap in our understanding of the N_2O budget. The isotopic compositions are reported as $\delta^{17}O$ and $\delta^{18}O$, and we define them as

$$\delta^{17}O(N_2O) = \frac{2\left[N_2^{17}O\right]/\left[N_2^{16}O\right]}{\left[^{16}O^{17}O\right]/\left[^{16}O^{16}O\right]} - 1 \quad (1)$$

$$\delta^{18}O(N_2O) = \frac{2\left[N_2^{18}O\right]/\left[N_2^{16}O\right]}{\left[^{16}O^{18}O\right]/\left[^{16}O^{16}O\right]} - 1. \quad (2)$$

[3] Unless otherwise stated, the δ values reported in this paper are referenced relative to atmospheric O_2, rather than the more commonly employed Vienna Standard Mean Ocean Water (V-SMOW). The magnitudes of the atmospheric $\delta^{17}O(O_2)$ and $\delta^{18}O(O_2)$ are 11.75 and 23.5‰ referenced to V-SMOW, respectively, while the values are zero as referenced to O_2 itself. The unit ‰ reads per mil or one part in thousand. The mass-dependent isotopic fractionation follows

$$\delta^{17}O \approx 0.515\ \delta^{18}O. \quad (3)$$

[4] The oxygen anomaly is defined as the residual from the above equation, or

$$\Delta^{17}O \approx \delta^{17}O - 0.515\ \delta^{18}O. \quad (4)$$

[5] It was discovered that tropospheric N_2O samples [*Cliff and Thiemens*, 1997] have $\Delta^{17}O \approx 1$. Subsequent measurements [*Cliff et al.*, 1999; *Röckmann et al.*, 2001] confirmed and extended the result into the stratosphere. The latter reference gives $\Delta^{17}O = 1.0 \pm 0.2$‰ at $\delta^{18}O = 20.7 \pm 0.3$‰.

[6] Several chemical processes have been proposed to explain this anomaly: $NO_2^*/NO_3^* + N_2$ [*Zellner et al.*, 1992], $CO_3^* + N_2$ [*McElroy and Jones*, 1996], $O(^1D) + N_2$ [*Estupiñán et al.*, 2002], $O_3^* + N_2$ [*Zipf and Prasad*, 1998; *Prasad*, 2002, 2005], $NH_2 + NO_2$ [*Röckmann et al.*, 2001], and $N + NO_2$ [*McLinden et al.*, 2003]. These processes have been summarized and discussed by *McLinden et al.* [2003] and *Kaiser and Röckmann* [2005]. In addition to the aforementioned proposals that generate nonzero $\Delta^{17}O$ in the atmosphere, it has also been suggested that microbial production of N_2O in the biosphere [*Michalski et al.*, 2003; *Kaiser et al.*, 2004; *Kaiser and Röckmann*, 2005] could contribute the observed oxygen anomaly. A recent calculation by *Kaiser and Röckmann* [2005] suggests that microbial nitrification and denitrification, $O(^1D) + N_2$, and NH_2 (and N) + NO_2 contribute 0.30, 0.36, and 0.18‰ to $\Delta^{17}O$, respectively, summing to a total of $0.82^{+0.30}_{-0.24}$‰. Biomass burning and industrial processes only make a small contribution to $\Delta^{17}O$.

[7] The essence of the above mechanisms is to transfer a heavy oxygen atom originally in O_3 to N_2O. It is known that atmospheric O_3 is enriched in heavy isotopologues

[1]Research Center for Environmental Changes, Academia Sinica, Taipei, Taiwan.
[2]Division of Geological and Planetary Sciences, California Institute of Technology, Pasadena, California, USA.

0148-0227/07/2006JD007876

Table 1. Summary of Reactions for the Production of Atmospheric N_2O[a]

Mechanism[b]	Reactions	Production(N_2O)
A	JPL06 recommended reactions	
	$O(^1D) + N_2 + M \rightarrow N_2O + M$	
$\Rightarrow$	$4.24 \times 10^{-34} T^{-0.88} [O(^1D)][N_2][M]$	4.1×10^7
B	Prasad's interpretation	
B1	$O(^1D) + O_3 \rightarrow O_3^*(^3B_1) + O(^3P)$	
	$O_3^*(^3B_1) + N_2 \rightarrow N_2O + O_2$	
$\Rightarrow$	$\phi_0 [O(^1D)][O_3][N_2](1.2 \times 10^{-10} / 9.65 \times 10^{15})$[c]	6.0×10^3
B2	$O_3 + h\nu \rightarrow O_3^*(^1B_2)$	
	$O_3^*(^1B_2) + N_2 \rightarrow N_2O + O_2$	
$\Rightarrow$	$\phi_1 [O_3][N_2]$	5.3×10^7
B3	$O(^1D) + N_2 + M \rightarrow N_2O + M$	
$\Rightarrow$	$\phi_2 (1.2 \times 10^{-11} \exp(110/T)[O(^1D)][N_2])$[d]	8.9×10^5
Kaiser and Röckmann [2005]	$NH_3 + OH \rightarrow NH_2 + H_2O$	
	$NH_2 + NO_2 \rightarrow N_2O + H_2O$	1×10^7
McLinden et al. [2003]	$NO + h\nu \rightarrow N + O$	
	$N + NO_2 \rightarrow N_2O + O$	3×10^6

[a]For this particular model, the tropospheric O_3 level is about 20–30 ppbv. Production (N_2O) denotes the column integrated N_2O production rate (molecules cm^{-2} s^{-1}). The surface steady state N_2O upwelling flux is taken to be 1.9×10^9 molecules cm^{-2} s^{-1} (or 14.3 TgN/year), which gives a tropospheric N_2O abundance ~320 ppbv; the flux is about ~10% lower than 16.4 TgN/year reported in *IPCC* [2001], because the present atmosphere is not in steady state. The conversion factor from molecules cm^{-2} s^{-1} to TgN/year is 7.52×10^{-9}. Note that densities used in the expression are in units of cm^{-3}.

[b]The arrows indicate the expressions used for the production of N_2O in the model.

[c]The value 1.2×10^{-10} is the rate coefficient of the reaction $O(^1D) + O_3 \rightarrow 2\ O_2$. The division by 9.65×10^{15} is to account for that ϕ_0 was obtained for this O_3 concentration.

[d]The product of $1.2 \times 10^{-11} \exp(110/T)[O(^1D)][N_2]$ represents the quenching rate of $O(^1D)$ with N_2.

and isotopomers with mass-independent fractionation [*Mauersberger*, 1987; *Krankowsky et al.*, 2000; *Mauersberger et al.*, 2001; *Lämmerzahl et al.*, 2002; *Brenninkmeijer et al.*, 2003; *Thiemens*, 2006]. The isotopic composition of atmospheric O_3 [*Liang et al.*, 2006] can be well explained by two processes: formation [*Thiemens and Heidenreich*, 1983; *Mauersberger et al.*, 1999; *Gao and Marcus*, 2001] and photolysis [*Johnson et al.*, 2001; *Bhattacharya et al.*, 2002; *Blake et al.*, 2003; *Liang et al.*, 2004; *Miller et al.*, 2005; *Prakash et al.*, 2005]. We briefly summarize the basic features of the O_3 isotopic anomaly. The isotopic enrichment is primarily caused by the formation of O_3. As a consequence of finite lifetime of O_3 complex in the intermediate state, symmetric molecules in their intermediate states tend to have greater deviation from their statistical density of states, compared with asymmetric isotopomers. This deviation is known as the "η effect" [e.g., see *Gao and Marcus*, 2001]. This formation process results in $\delta^{49}O_3 \approx \delta^{50}O_3 \approx 100‰$, relative to atmospheric O_2. In addition, about 10% of the observed O_3 isotopic enrichment is due to photolytic processes. The photolysis effect provides an explanation for the observed altitude variation of the O_3 isotopic composition in the stratosphere. See *Liang et al.* [2006] for details.

[8] In this paper, we simulate the isotopic fractionation of O_3 and N_2O in one-dimensional (height) and two-dimensional (latitude and height) modes. The modeling of the longitudinal variation requires a three-dimensional model and will be deferred to a later paper. The calculated isotopic composition of O_3 is then used to evaluate new sources of N_2O and their associated oxygen anomaly. The paper is organized as follows. We summarize in section 2 a new interpretation [*Prasad*, 2002, 2005] of the laboratory measurements of the N_2O quantum yield in the mixture of $O_3/O_2/N_2$. To provide deeper insight into the physics of new N_2O sources, one-dimensional model results are presented and discussed in detail in section 3. The two-dimensional simulations that extend the results of one-dimensional models are shown in section 4. Implications for paleoatmospheric O_3 and concluding remarks are presented in section 5.

2. Sources of N_2O

[9] The current globally averaged surface abundance of N_2O is ~320 ppbv, with a few parts per billion by volume more in the Northern Hemisphere than in the Southern Hemisphere. Several known sources of N_2O are reported in IPCC report [*Intergovernmental Panel on Climate Change* (*IPCC*), 2001], summing to a total emission of 16.4 TgN/year or 2.2×10^9 molecules cm^{-2} s^{-1}; about half of N_2O is emitted naturally and the rest is produced by anthropogenic activities. (The conversion factor for N_2O emission from molecules cm^{-2} s^{-1} to TgN/year is 7.52×10^{-9}.) The identified major sinks for N_2O are photolysis (90%) and the reaction with $O(^1D)$ (10%). Both reactions occur primarily in the stratosphere, resulting in a lifetime of ~120 years for N_2O. Consequently, there are only small vertical and horizontal gradients in N_2O in the troposphere.

[10] Isotopic measurements have been used to constrain the global N_2O budget. The observed $\delta^{15}N$ and $\delta^{18}O$ are 7.0 and 20.7‰ [*Kim and Craig*, 1993] relative to atmospheric N_2 and O_2, respectively. The atmospheric cycle of N_2O is as follows. Tropical rain forest, fertilized soils, and ocean are major source regions in the troposphere. Compared with the mean tropospheric values, the land source is strongly depleted in ^{15}N and ^{18}O; the oceanic source is moderately depleted. The back flux of N_2O from the stratosphere is highly enriched in both ^{15}N and ^{18}O. The budget of the isotopologues and isotopomers of N_2O is nearly balanced.

[11] The discovery of mass-independent oxygen anomaly in N_2O [*Cliff and Thiemens*, 1997; *Cliff et al.*, 1999; *Röckmann et al.*, 2001] suggests that its sources and sinks have not yet been completely understood. Several mechanisms that transfer heavy oxygen atom from O_3 to N_2O have

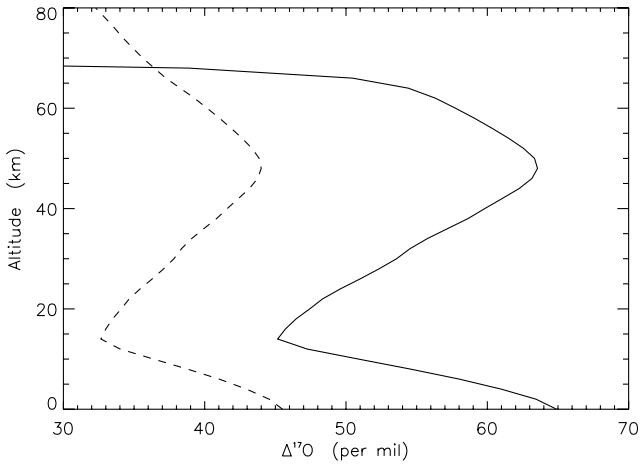

Figure 1. Vertical profiles of $\Delta^{17}O$ for O_3 (dashed) and $O(^1D)$ (solid).

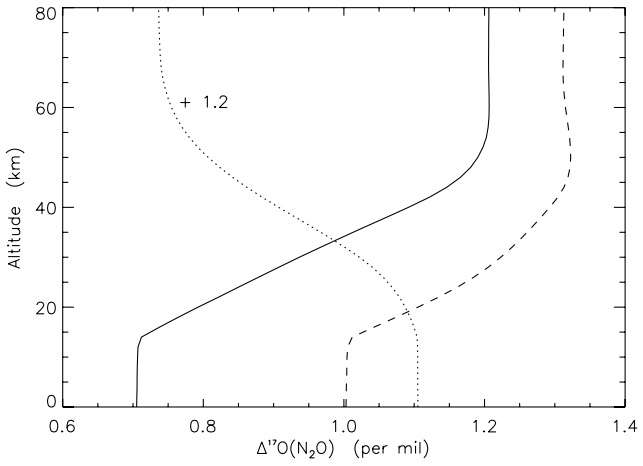

Figure 3. Vertical profiles of $\Delta^{17}O$ for N_2O from two processes: $O(^1D) + N_2$ (solid; mechanism A) and $O_3^* + N_2$ (dashed; mechanism B). A case for which atmospheric N_2O sources vanish is shown by the dotted line. For best visualization, a constant value of 1.2 is added to the dotted line. See text for negative values.

been proposed (see above). Of these proposals, the reactions of N_2 with $O(^1D)$ and O_3 are supported by laboratory measurements [*DeMore and Raper*, 1962; *Gaedtke et al.*, 1972; *Kajimoto and Cvetanovic*, 1976; *Maric and Burrows*, 1992; *Estupiñán et al.*, 2002]. These processes provide a new source of N_2O in the atmosphere, contrary to the current belief that the source of N_2O in the atmosphere is negligible. The mechanism [*Yung et al.*, 2004] that exchanges O atoms, $Q(^1D) + N_2O \rightarrow O + N_2Q$, where $Q = {}^{18}O$ or ${}^{17}O$, has been ruled out by laboratory experiments [*Kaiser and Röckmann*, 2005].

[12] In this paper, we follow the recommendation of *Sander et al.* [2006, JPL06 hereafter] for the production of N_2O from $O(^1D) + N_2$ [*Estupiñán et al.*, 2002]. The JPL06 recommended reaction and the rate coefficient are taken to be our reference model and are denoted as mechanism A (Table 1). We also consider the interpretation of *Prasad* [2002, 2005], denoted as mechanism B, in which O_3 in its excited state reacting with N_2, instead of $O(^1D) + N_2$, dominates the production of N_2O in the atmosphere. Prasad's interpretation is briefly described below.

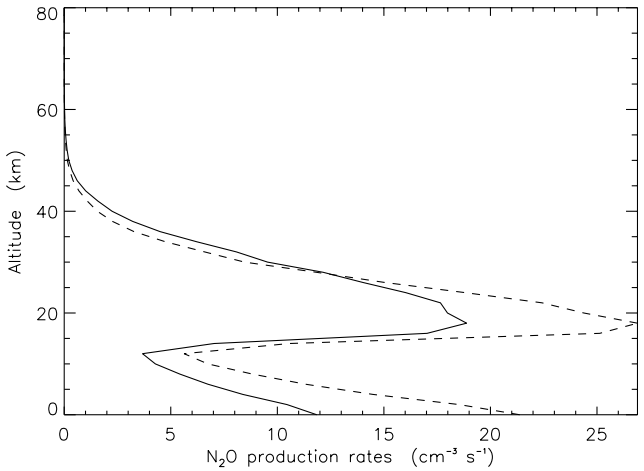

Figure 2. Production rates of N_2O by the reactions of $O(^1D) + N_2$ (solid; mechanism A, reference model) and $O_3^* + N_2$ (dashed; mechanism B). The tropospheric O_3 concentration is ~20–30 ppbv.

[13] The measurements of *Estupiñán et al.* [2002] were taken under atmospheric conditions, i.e., pressure spanning from ~100 to 1000 mbar and temperature from 220 to 324 K. The previous measurements [*Kajimoto and Cvetanovic*, 1976] of N_2O quantum yield were performed at much higher pressures (27–110 bar). Incorporating the measurements of the N_2O quantum yield in the solution of the mixture of O_3 and N_2 [*DeMore and Raper*, 1962], *Prasad* [2005] proposed a three-component model for the density ($[M]$) and temperature (T) dependence of the N_2O quantum yield, $\phi(N_2O)$:

$$\phi(N_2O) = \phi_0 + \phi_1 + \phi_2, \tag{5}$$

where ϕ_0 represents the contribution from vibrationally and electronically excited O_3, $O_3^*(^3B_1)$, and has no density dependence ($[M]^0$), ϕ_1 represents electronically excited O_3, $O_3^*(^1B_2)$, and is a linear function of density ($[M]^1$), and ϕ_2 denotes the reaction of $O(^1D) + N_2$ which has a squared dependence on density ($[M]^2$). The functional forms of ϕ_0, ϕ_1, and ϕ_2 are

$$\phi_0 = 5.63 \times 10^{-5} \exp(-1899/T) \tag{6}$$

$$\phi_1 = 6.99 \times 10^{-26} \chi [M] \Lambda(\lambda) \tag{7}$$

$$\phi_2 = \left(\frac{2.95}{T}\right)^{0.6} \chi \left(3.86 \times 10^{-26}[M] + \frac{[M]}{[M] + 1.98 \times 10^{24}}\right) \times \left(\frac{[M]}{[M] + 8.98 \times 10^{20}}\right), \tag{8}$$

where χ is the volume mixing ratio of N_2, which is about 0.8. ϕ_2 has wavelength dependence, $\Lambda(\lambda)$, which is unity at wavelengths <300 nm, climbs to ~5 at ~320 nm, and then

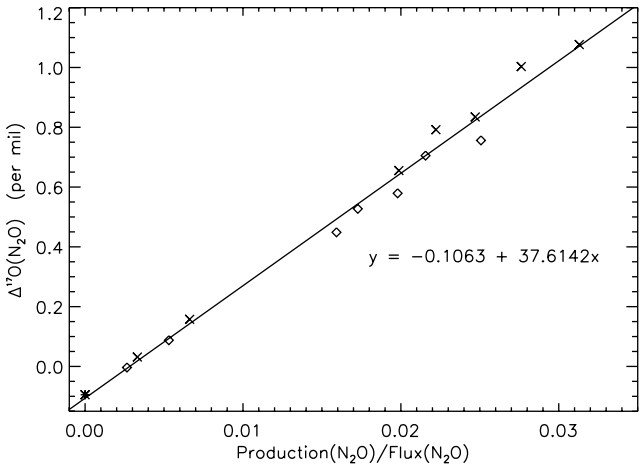

Figure 4. Sensitivity of the results to the changes of tropospheric O_3 abundances and surface N_2O fluxes. Diamonds and crosses represent the model results based on mechanisms A and B, respectively. Asterisks represent the case where atmospheric N_2O sources vanish. Solid line represents a least squares linear fit to the results: $y = -0.1063 + 37.6142x$.

drops at >320 nm [see Figure 2 of *Prasad*, 2002]. This wavelength dependent quantum yield of N_2O production is obtained by fitting the measurements performed in the liquid O_3/N_2 mixture [*DeMore and Raper*, 1962]. These mechanisms as well as some other proposed pathways are summarized in Table 1. The table shows that the mechanism of *McLinden et al.* [2003] is less significant, compared with the other three mechanisms.

[14] A one-dimensional model is used to evaluate the contribution from the aforementioned N_2O production pathways. The results are summarized in Table 1. It is shown that in Prasad's interpretation, ϕ_1 dominates the production of N_2O. Therefore in the following discussion, we focus on ϕ_1 as the source of N_2O in Prasad's mechanism.

3. One-Dimensional Model

[15] To demonstrate the influence of the introduction of these new atmospheric N_2O sources, we first focus on one-dimensional modeling. The model is based on our previous papers on O_3 [*Liang et al.*, 2006] and CO_2 [*Liang et al.*, 2007] isotopic simulations. The profiles of $\Delta^{17}O(O_3)$ and $\Delta^{17}O(O(^1D))$ are shown in Figure 1. The small $\Delta^{17}O(O(^1D))$ above ~70 km is caused by O_2 Lyman-α photolysis [see *Liang et al.*, 2007]. The $\Delta^{17}O(O_3)$ near the surface used here is greater than the reported values of 20–35‰ [e.g., *Johnston and Thiemens*, 1997]. We note that the difference between model and observations could be reduced by applying more accurate temperature and pressure-dependent formation rates for O_3 isotopomers and isotopologues, which are currently not available. Even though our model is less satisfactory in the troposphere, our study on N_2O would not be seriously affected, because >2/3

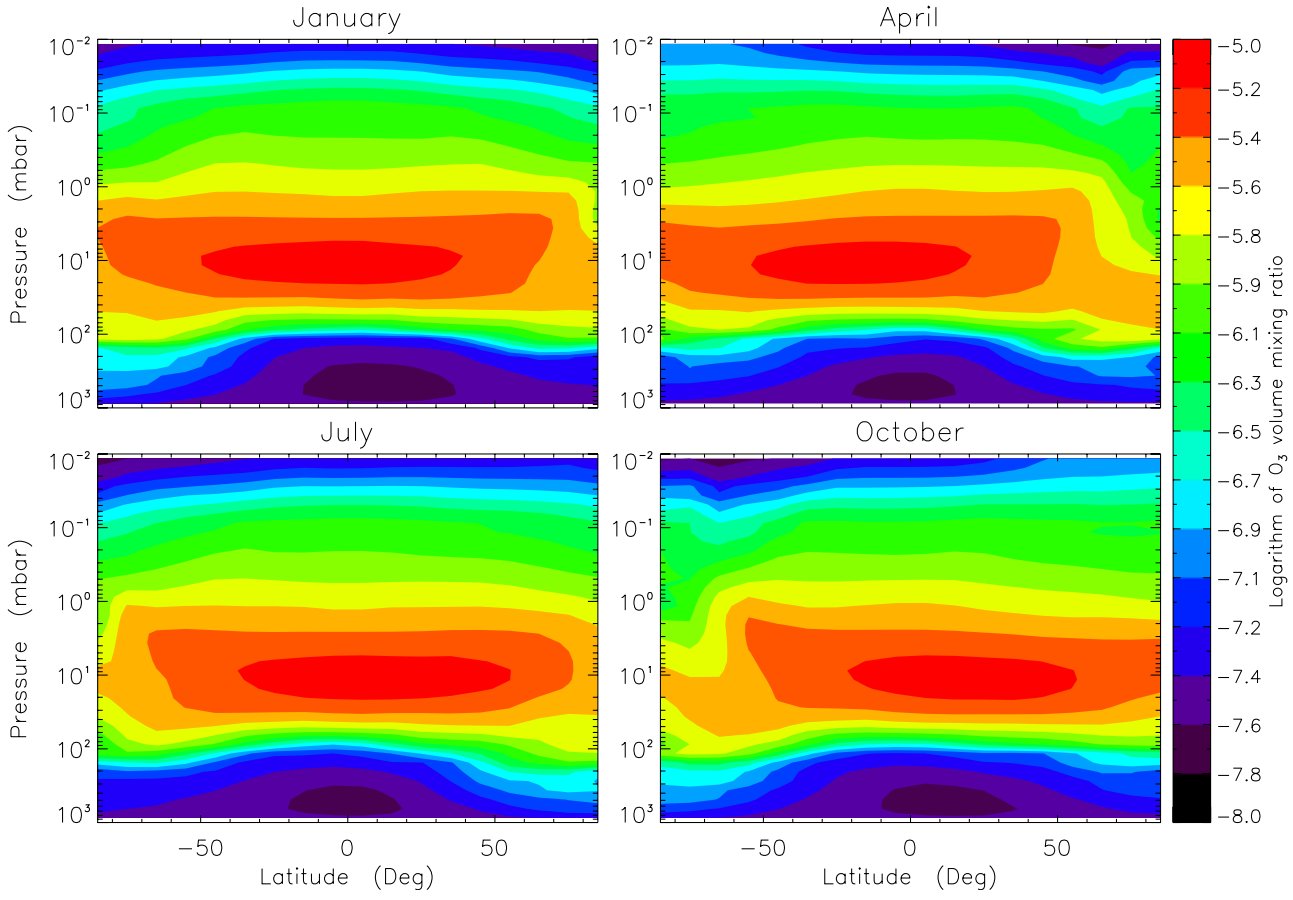

Figure 5. Latitude-pressure plots of O_3 volume mixing ratios for January, April, July, and October.

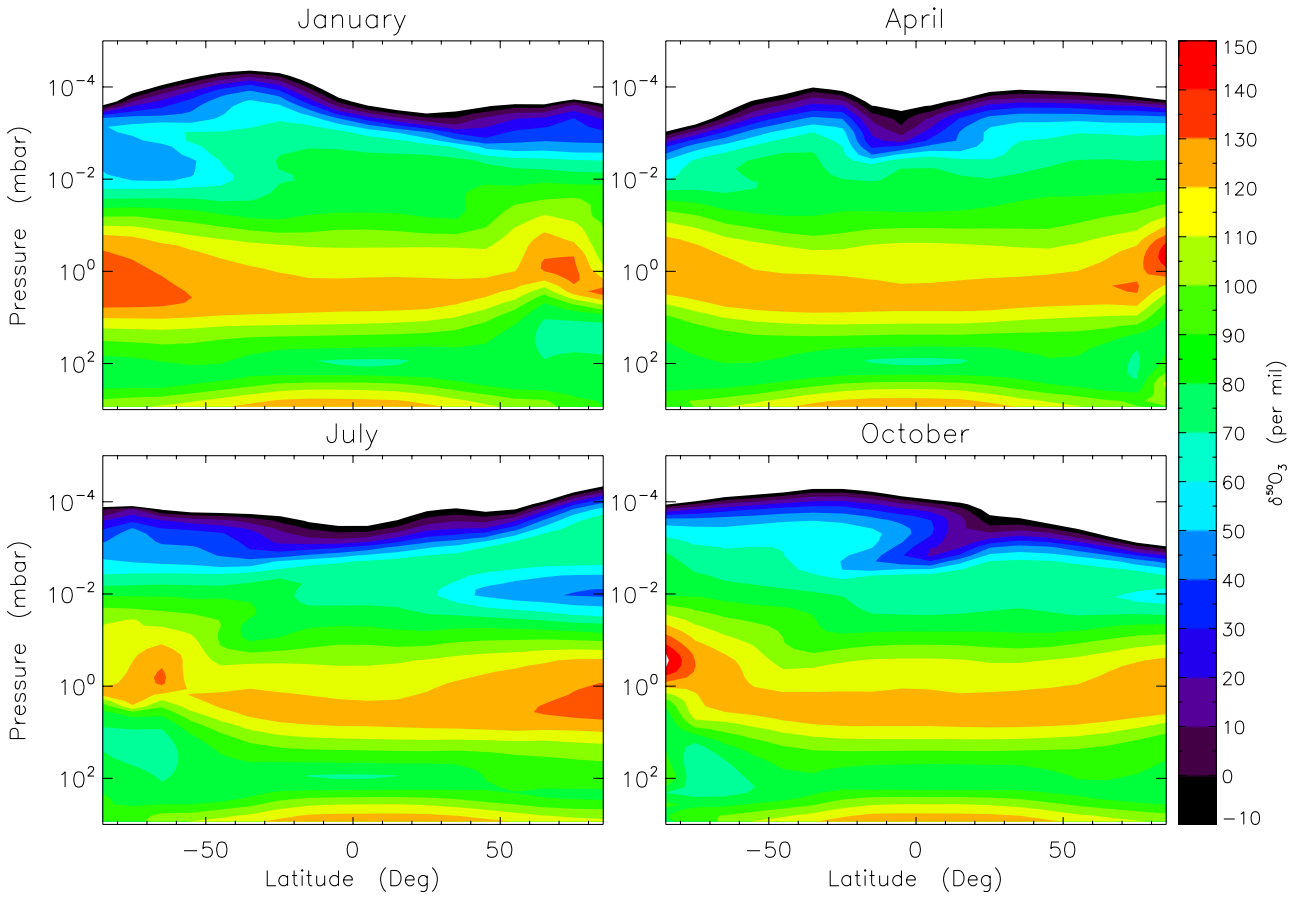

Figure 6. Same as Figure 5 for $\delta^{50}O_3$.

of the atmospheric sources of N_2O are in the stratosphere, where our current model can well reproduce the observed isotopic composition of O_3 [see *Liang et al.*, 2006]. An error <50% in the modeled isotopic composition in the tropospheric O_3 results in an error <17% for the $\Delta^{17}O$ in the new source of N_2O.

[16] Figure 2 shows the production rates of new N_2O sources due to two processes: $O(^1D) + N_2$ (solid; mechanism A) and $O_3^* + N_2$ (dashed; mechanism B), where O_3^* is produced by the photolysis of O_3 in the Hartley-Huggins band (see section 2). The column integrated production rates of N_2O from these two processes are 4.1×10^7 (0.3 TgN/year) (mechanism A) and 5.3×10^7 (0.4 TgN/year) (mechanism B) molecules cm^{-2} s^{-1}. The atmospheric N_2O source constitutes about 2% of the total N_2O source, $\sim 2 \times 10^9$ molecules cm^{-2} s^{-1} needed to maintain the surface N_2O concentration of ~320 ppbv in steady state. [The surface flux (1.9×10^9 molecules cm^{-2} s^{-1}) used here is slightly less (~10%) than the *IPCC* [2001] value, because the present atmosphere is not in steady state.] This suggests that the isotopic anomaly originally in $O(^1D)$ or O_3 is diluted by a factor of ~50 when transferred to N_2O. For $\Delta^{17}O = 50‰$ in $O(^1D)$ or O_3, we expect that $\Delta^{17}O$ in N_2O is 1‰.

[17] Calculated profiles of $\Delta^{17}O$ for N_2O are presented in Figure 3. In this model, the tropopause is at 14 km. Below 14 km, high eddy mixing causes the value of $\Delta^{17}O$ to be nearly uniform. The sharp increase above 14 km is due to the enhancements of N_2O production in the stratosphere and the weak stratosphere-troposphere exchange. As the destruction of N_2O is characterized by a linear loss mechanism, the fractionation of isotopically substituted N_2O can be considered as a Rayleigh fractionation process, which is

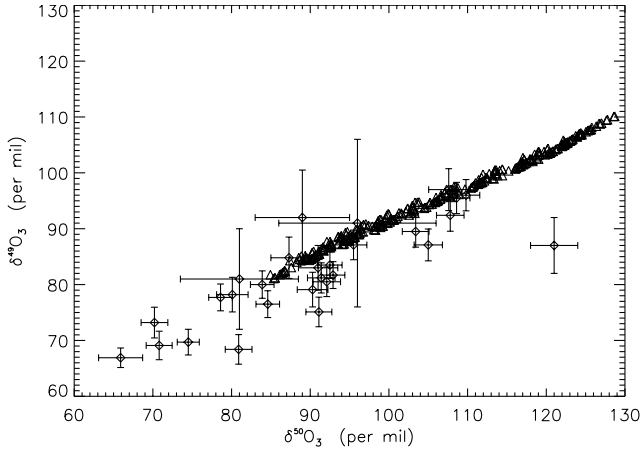

Figure 7. Three-isotope plot of ozone. Diamonds are balloon-borne mass spectrometer measurements [*Krankowsky et al.*, 2000; *Mauersberger et al.*, 2001; *Lämmerzahl et al.*, 2002]. The error bars in the atmospheric measurements are for 1σ. The two-dimensional model results at similar altitudes and reasons as the atmospheric measurements are shown by the triangles.

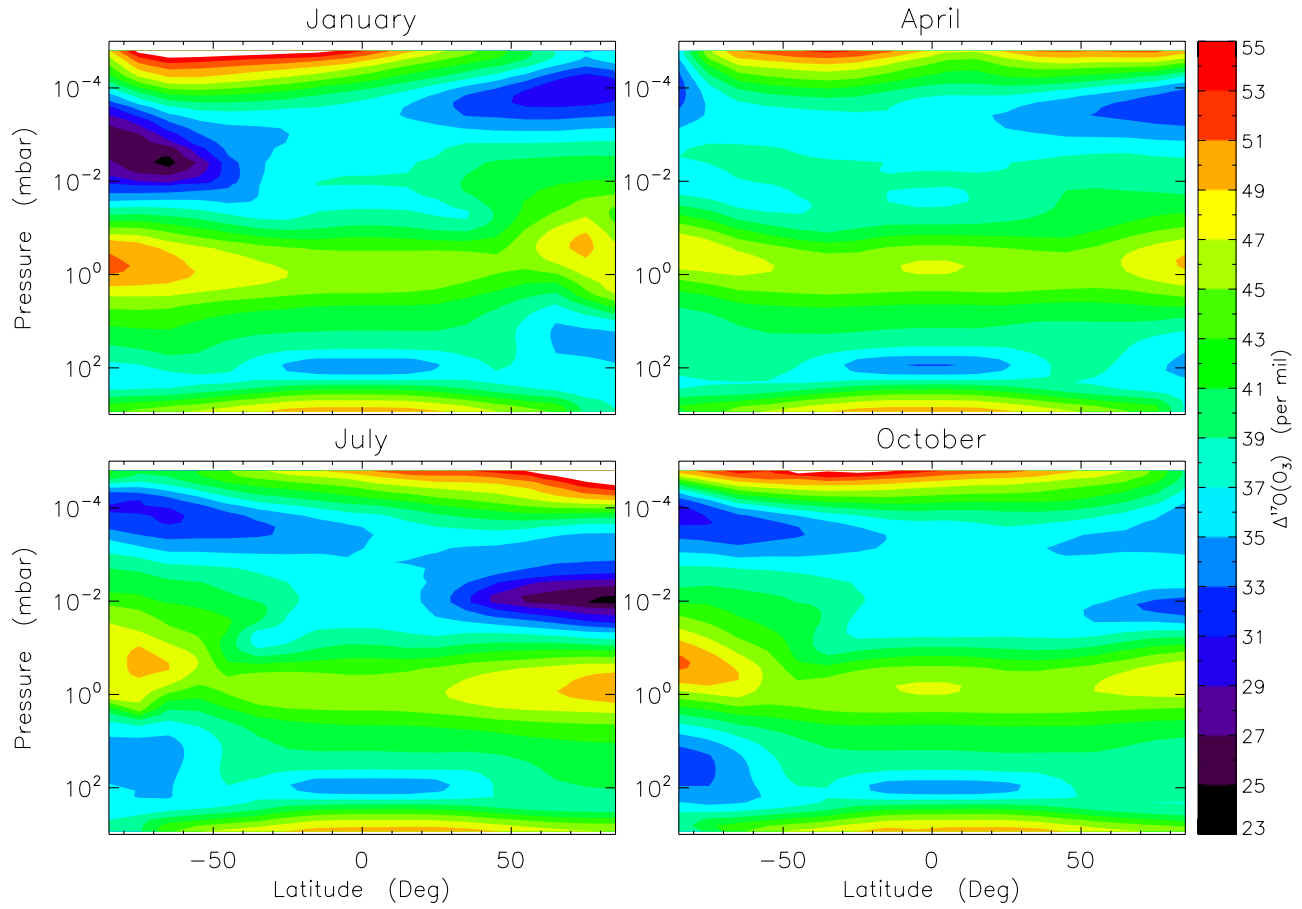

Figure 8. Same as Figure 5 for $\Delta^{17}O(O_3)$ model.

described by the following formula [e.g., see *Morgan et al.*, 2004 for details]:

$$ln\left(\frac{1+\delta_i}{1+\delta_{i,0}}\right) = \epsilon_i ln(f), \tag{9}$$

where δ_i is the δ for species i, $\delta_{i,0}$ is the initial δ, ϵ_i is the fractionation factor caused by photolysis (see *Liang et al.* [2004] for a more detail definition and discussion for ϵ factor), and f is the ratio of the remaining N_2O to that of the initial N_2O in the air parcel. When δ is small, δ is a linear function of ϵ:

$$\delta_i \approx \delta_{i,0}\epsilon_i ln(f). \tag{10}$$

[18] In this paper, we assume an ϵ for $N_2^{17}O$ that is 0.515 times that for $N_2^{18}O$, consistent with laboratory measurements [e.g., *Kaiser et al.*, 2004]. This implies that $\delta^{17}O(N_2^{17}O) \approx 0.515\ \delta^{18}O(N_2^{18}O)$. When the δ value of N_2O is as high as ~100‰, the linear approximation [equation (10)] no longer holds. To minimize the nonlinearity between δ and ϵ, we use the full expression in equation (9) to calculate $\Delta^{17}O$, namely

$$\Delta^{17}O(N_2O) = \delta^{17}O - \left[\left(1+\delta^{18}O\right)^{0.515} - 1\right]. \tag{11}$$

[19] Though this equation can account for the nonlinearity between δ and ϵ, it has a curious effect in that $\Delta^{17}O(N_2O)$ does not vanish when the atmospheric N_2O source is zero (dotted line in Figure 3). This is due primarily to the selection of the reference (O_2 here) in which the isotopic ratios deviate from the ratios in the target samples. For example, in the atmospheric N_2O, the back flux of the stratospheric N_2O enhances the tropospheric $\delta^{18}O$ in $N_2^{18}O$ by ~15‰. So $\ln(1+\delta^{18}O) - \delta^{18}O \approx -0.1$‰, which is still within the statistical error bar of the measurements of 0.2‰ [e.g., *Röckmann et al.*, 2001]. The value decreases with $\delta^{18}O$ or altitude (see Figure 3).

[20] To gain insight into the impact of the new sources, we vary tropospheric O_3 abundance and the flux of surface N_2O sources. The sensitivity of the results to these changes is summarized in Figure 4. It is shown that the oxygen anomaly of N_2O increases with the contribution from atmospheric N_2O sources. Note that under the same condition the reaction of O_3^* and N_2 (mechanism B) tends to produce more N_2O and hence greater $\Delta^{17}O$ anomaly (~0.3‰; Figure 3), compared with that of $O(^1D) + N_2$ (mechanism A). This is caused by $\Lambda(\lambda)$ [equation (7)] that enhances the N_2O production at longer wavelengths where heavy O_3 is more enriched. For similar N_2O production, $\Delta^{17}O$ anomaly from the mechanism B is about 0.1‰ in excess of the mechanism A (Figure 4).

4. Two-Dimensional Simulation

[21] To provide a direct comparison with atmospheric measurements, two-dimensional modeling is performed.

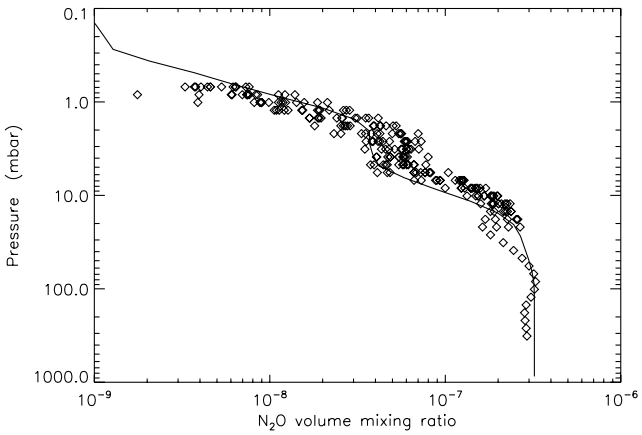

Figure 9. Comparison of observed (diamonds) and modeled (solid) concentrations of N_2O in the terrestrial atmosphere for March at 15°N. The observations are from the Atmospheric Trace Molecule Spectroscopy Experiment (ATMOS) campaigns [e.g., see *Morgan et al.*, 2004].

Two-dimensional models are sufficient in the stratosphere, where the longitudinal variation is insignificant. Since the N_2O lifetime is long, two-dimensional modeling is a good approximation for this work. See *Morgan et al.* [2004] for details about the two-dimensional model.

[22] The isotopic composition of atmospheric O_3 is critical to modeling the oxygen anomaly in atmospheric N_2O. To account for the O_2 Lyman-α photolysis [*Liang et al.*, 2007] in the mesosphere, we calculate the isotopic composition of O_3 up to ~130 km, which is higher than our previous two-dimensional models of ~80 km [e.g., *Morgan et al.*, 2004]. The horizontal and vertical eddy mixing coefficients are taken from *Summers et al.* [1997]. The two-dimensional advection and zonally averaged temperature are derived from the Whole Atmosphere Community Climate Model (WACCM; data available on the Website http://waccm.acd.ucar.edu/) 3-hourly outputs [*Sassi et al.*, 2002, 2004]. We follow the same technique as in the work of *Jiang et al.* [2004] to derive the residual circulations [*Andrews et al.*, 1987] needed for transport. The eddy diffusion coefficients, residual circulation, and temperature are then monthly averaged. The WACCM model outputs (winds and temperature) are used only to derive the profiles of O_3 and $O(^1D)$. For the simulation of N_2O, we use the same atmospheric transport and temperature profiles as that in the work of *Morgan et al.* [2004]. This is to provide a better comparison with our previous N_2O work [*Morgan et al.*, 2004]. Comparisons between atmospheric circulations will be demonstrated in a later paper (Liang et al., Seasonal cycle of $C^{16}O^{16}O$, $C^{16}O^{17}O$, and $C^{16}O^{18}O$ in the middle atmosphere: Implications for mesospheric dynamics and the biogeochemical sources and sinks of CO_2, submitted to Journal of Geophysical Research: Atmosphere, 2007, hereinafter referred to as Liang et al., submitted manuscript, 2007) which studies the isotopic composition of CO_2. The

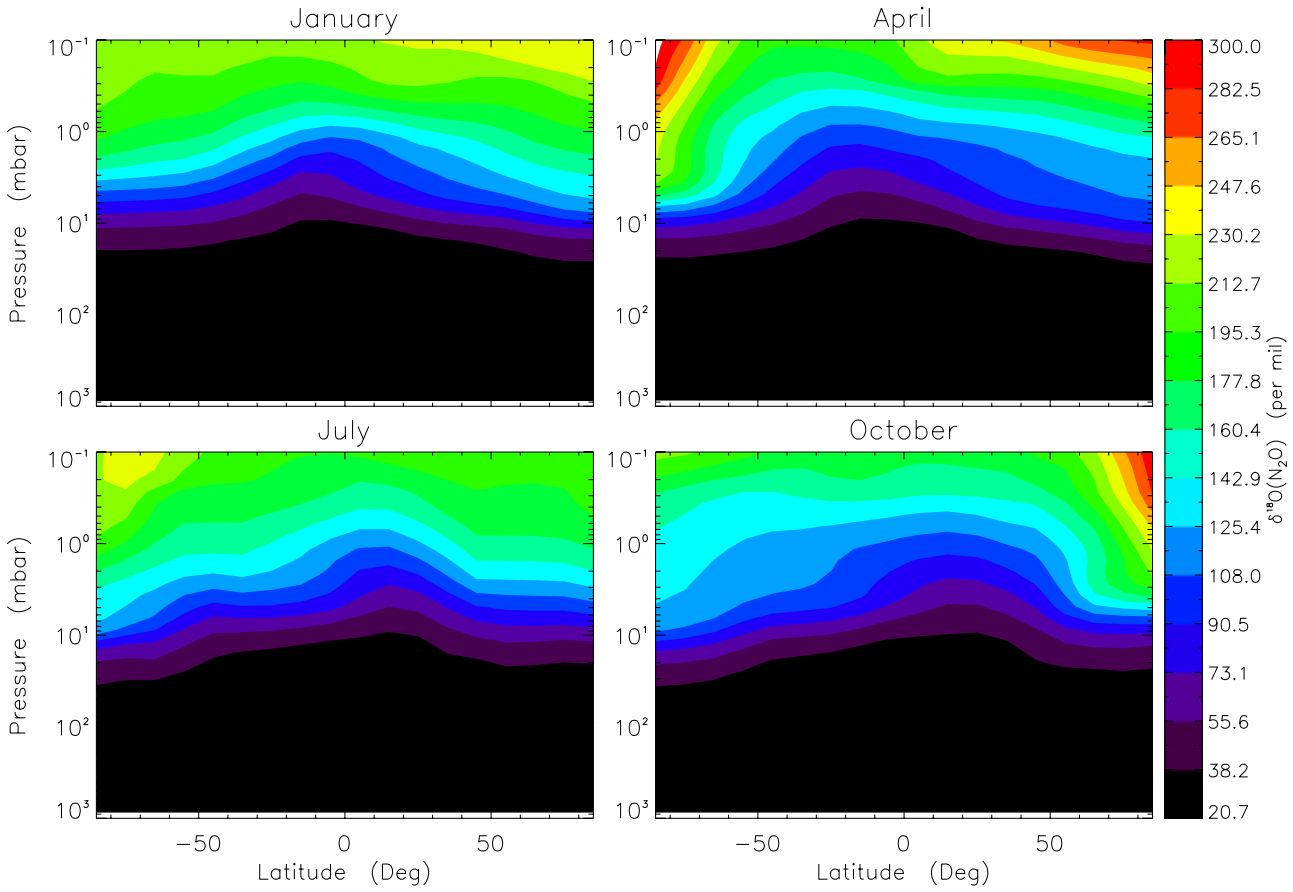

Figure 10. Same as Figure 5 for $\delta^{18}O(N_2O)$ (mechanism A).

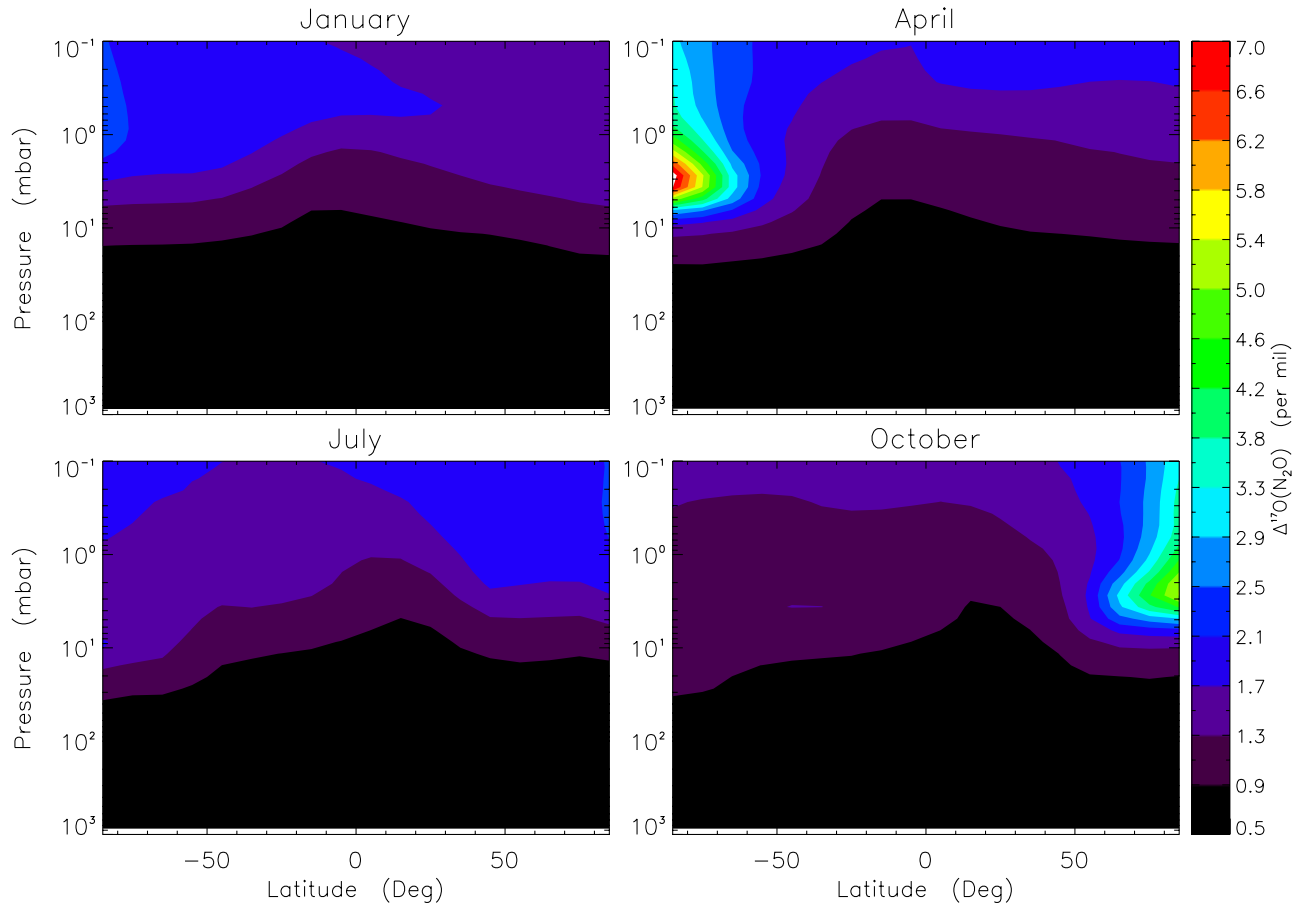

Figure 11. Same as Figure 5 for $\Delta^{17}O$ in N_2O (mechanism A).

reason why we can use different circulations and different temperature profiles to simulate O_3 and N_2O is that O_3 and $O(^1D)$ are both short-lived, compared to dynamical transport, and their isotopic composition is insensitive to the variation of temperature ($\sim$0.6‰ K^{-1}).

[23] Simplified oxygen chemistry is taken from the work of *Liang et al.* [2006]. The model is adjusted (with prescribed catalysts for the destruction of O_3) in order to match the climatological O_3 profiles in the middle atmosphere. In the troposphere, our simplified oxygen chemical model does a less satisfactory job, because NO_x (NO and NO_2) chemistry is the major source of O_3 in the troposphere and it is not included in the current model. We scale our calculated O_3 concentration in the troposphere to match the climatological abundances [see, e.g., *Morgan et al.*, 2004]. The same scaling factor is applied to the abundances of the isotopologues and isotopomers of O_3 and $O(^1D)$. This scaling does not affect our calculation, as we assume that the isotopic fractionation is caused only by the formation and photolysis of O_3.

[24] The calculated profiles of the abundance and the isotopic composition of O_3 are presented in Figures 5 and 6, respectively. This represents a generalization for our previous one-dimensional modeling [*Liang et al.*, 2006]. It is shown that the seasonality of $\delta^{50}O_3$ is weak at low latitudes, consistent with temperature seasonality. Above the homopause ($\sim$90 km, or $\sim10^{-3}$ mbar), the depletion of $\delta^{50}O_3$ is caused by diffusive separation. Figure 7 shows the three-isotope plot of oxygen for O_3, consistent with the results obtained previously [*Liang et al.*, 2006] that the model overestimates the δ values of ozone by about 20‰, i.e., biased too high by $\sim$20%. Further laboratory measurements of the formation rates of O_3 isotopomers and isotopologues at atmospheric conditions are needed in order to resolve the bias.

[25] Figure 8 shows the calculated $\Delta^{17}O$ in O_3. The anomaly is on the order of 50‰. To explain the observed 1‰ oxygen anomaly in N_2O, the atmospheric source of N_2O needs to be about 2% of the total source, i.e., a column production of $N_2O \sim 5 \times 10^7$ molecules cm^{-2} s^{-1} or 0.4 TgN/year, consistent with the suggestion by *Kaiser and Röckmann* [2005].

[26] With this simplified model, the calculated N_2O abundance (Figure 9) above $\sim$20 mbar altitude level is slightly lower than our previous work [cf. Figure 2 of *Morgan et al.*, 2004], but the value is still within the statistical variation of the observations. For comparison, the modeled $\delta^{18}O$ in N_2O is presented in Figure 10, which shows that the isotopic composition of $\delta^{18}O$ above $\sim$20 mbar level increases faster than previous models [*Morgan et al.*, 2004].

[27] We then calculate the $\Delta^{17}O$ of N_2O based on mechanism A, using the O_3 abundance in Figure 5 and

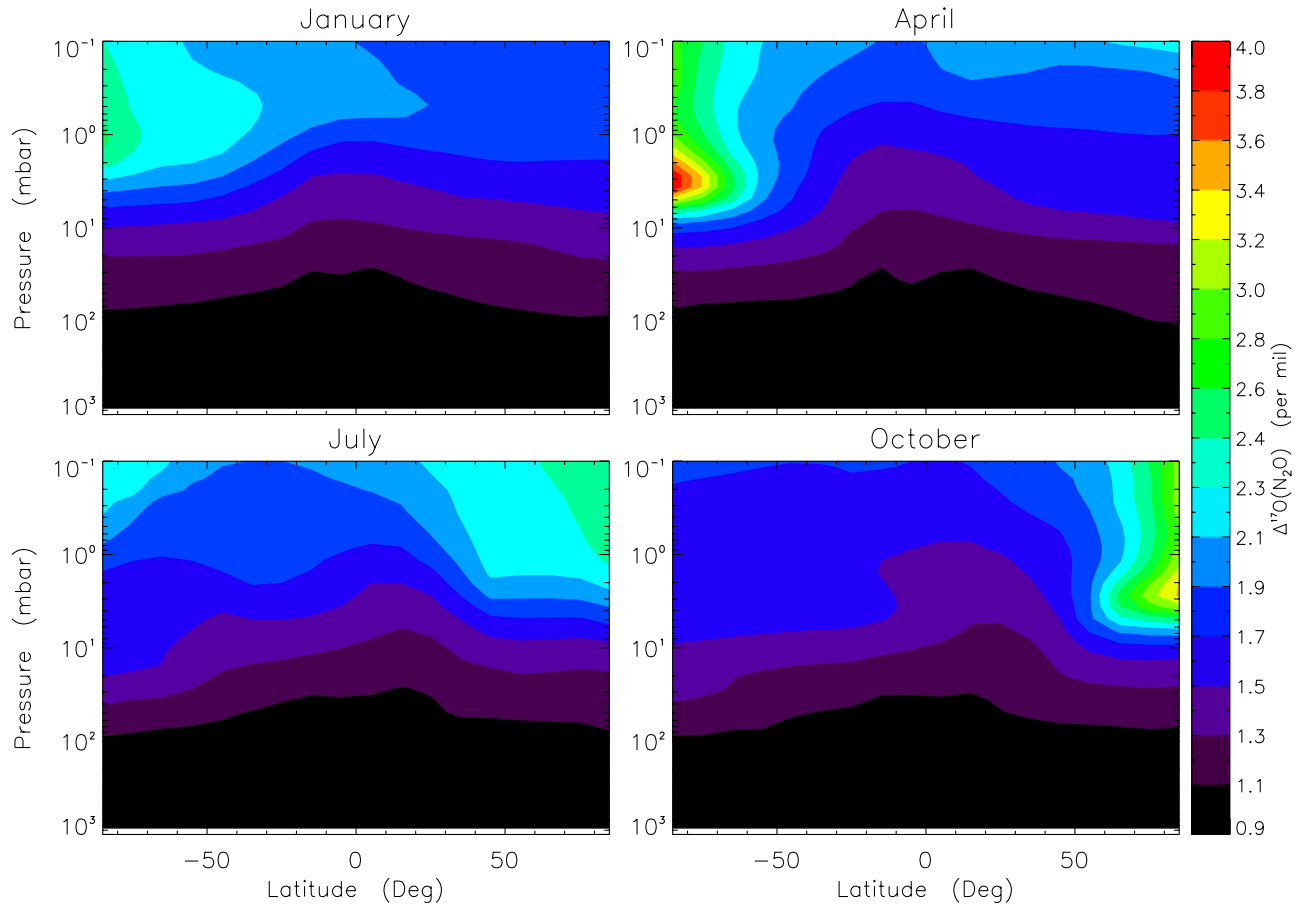

Figure 12. Same as Figure 5 for $\Delta^{17}O$ in N_2O (mechanism B).

$\Delta^{17}O(O_3)$ in Figure 8, and the result is shown in Figure 11. The averaged $\Delta^{17}O$ in tropospheric and lower stratospheric N_2O is 0.57‰. As described above, given an error <50% in the modeled isotopic composition in the tropospheric O_3 and 20% in the stratosphere, the error in the $\Delta^{17}O$ from the new source of N_2O is <30%, suggesting that the magnitude of the oxygen anomaly in N_2O produced by mechanism A is >0.40‰. For comparison, the result based on mechanism B

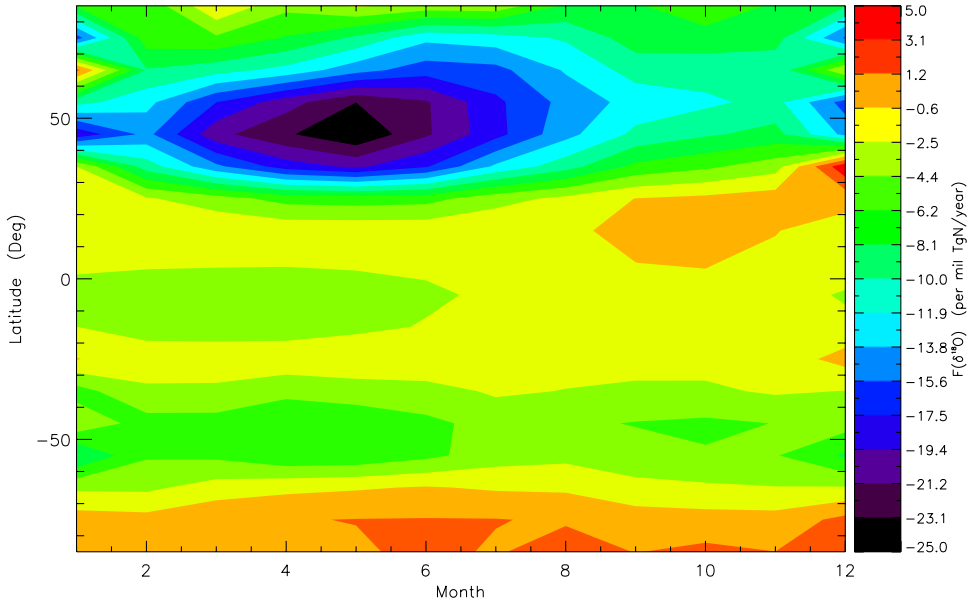

Figure 13. Seasonal cycle of the isoflux of $\delta^{18}O(N_2O)$ (F) across the tropopause. Values are in ‰TgN/year. Negative values denote downward flux.

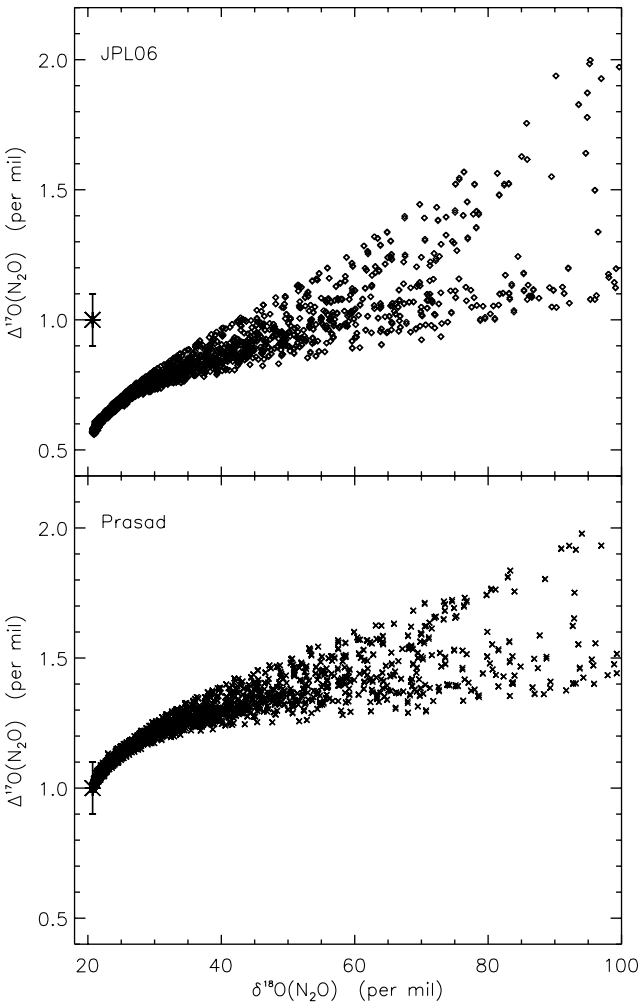

Figure 14. Scatterplot of $\Delta^{17}O$ and $\delta^{18}O$ in N_2O. Diamonds and crosses represent mechanisms A and B model results, respectively. The atmospheric measurements [*Röckmann et al.*, 2001] are shown by asterisks, with 1 σ reported statistical error bar overplotted.

is shown in Figure 12. Using this model, the calculated $\Delta^{17}O$ is 1.01 or >0.71‰ after accounting for a possible error in the tropospheric O_3.

[28] Finally, we update the isoflux of $\delta^{18}O$ of N_2O across the tropopause that was reported in our previous paper [*Morgan et al.*, 2004]. The results are shown in Figure 13. The stratospheric processes enhance the abundance of $N_2{}^{18}O$ relative to that in the troposphere. Negative values denote the isoflux is transported downward. The maximum downward isoflux appears at mid-latitudes of the summer Northern Hemisphere; a similar phenomenon has been seen in the isoflux of $\delta^{18}O(CO_2)$ (Liang et al., submitted manuscript, 2007). In this work, we follow the same definition (independent of season) of the tropopause as in the work of *Morgan et al.* [2004], in which the tropopause is approximately at 100 mbar between 30°S and 30°N, 200 mbar between 30° and 60°, and 300 mbar poleward of 60°. The global annual isoflux of $\delta^{18}O(N_2O)$ across the tropopause is −95.3‰ TgN/year, a factor of ~2 less than the value reported by *Morgan et al.* [2004]. This is because the tropopause was defined at 86 mbar (not 100 mbar) by *Morgan et al.* [2004] where the $\delta^{18}O$ of N_2O is greatly enhanced compared with that at lower altitudes at 100–200 mbar.

5. Discussion and Summary

[29] Sources of nonzero $\Delta^{17}O$ in atmospheric N_2O have long been a puzzle since its discovery in 1997 in tropospheric samples [*Cliff and Thiemens*, 1997]. Subsequent measurements [*Cliff et al.*, 1999; *Röckmann et al.*, 2001] confirmed the discovery and extended it to the stratosphere. The observed $\Delta^{17}O$ is ~1‰. To explain this anomaly, new atmospheric N_2O sources are proposed. This atmospheric N_2O source has to be about a few percent (Figure 4) of the sum of the anthropogenic and natural N_2O sources, contrary to the current belief that the atmospheric N_2O source is insignificant. Of the several proposed mechanisms for the new sources, the reactions of $O(^1D)$ [*Estupiñán et al.*, 2002] and O_3^* [*Prasad*, 2002, 2005] with N_2 dominate and are supported by recent laboratory measurements [*Estupiñán et al.*, 2002]. The former pathway is recommended by JPL06 [*Sander et al.*, 2006].

[30] Incorporating the proposed mechanisms into our two-dimensional models, we find that the $\Delta^{17}O$ in N_2O increases with altitude (Figures 11 and 12). We also find that the seasonality of $\Delta^{17}O$ is small at low latitudes but is significant at about 3 mbar in the polar regions. Future atmospheric measurements in these regions are needed to validate our model and to verify the existence of the new N_2O sources. Figure 14, which shows a scatterplot of $\Delta^{17}O$ and $\delta^{18}O$, provides a direct comparison to observations, illustrating that $\Delta^{17}O$ caused by mechanism A increases faster with $\delta^{18}O$ than that by mechanism B.

[31] To distinguish between mechanisms A and B, three tests are suggested. For atmospheric observations, the maximum seasonality of $\Delta^{17}O$ is about 6‰ for mechanism A but it is ~3.5‰ for mechanism B. In the laboratory, more measurements for the N_2O quantum yield in the mixture of $O_3/O_2/N_2$ are needed to be taken under conditions similar to the atmosphere (pressure ~10–1000 mbar, temperature ~200–300 K, and UV photons with wavelengths ~230–350 nm). If mechanism B is correct, the $\Delta^{17}O$ in N_2O and N_2O quantum yield have a stronger wavelength-dependence than that by mechanism A, especially in the Huggins band of O_3. One can also add CO_2 in laboratory samples. The isotopic composition of CO_2 is a powerful tracer for the abundance and the isotopic composition of $O(^1D)$ [see *Liang et al.*, 2007]. So an alternative way is to photolyze the $O_3/O_2/N_2$ mixture at Lyman-α. If mechanism A is preferred, one will observe a highly enriched heavy N_2O, similar to that in mesospheric CO_2 [*Liang et al.*, 2007; Liang et al., submitted manuscript, 2007].

[32] In summary, we have quantitatively modeled the isotopic composition of O_3 and N_2O in the atmosphere. The calculated $\Delta^{17}O$ of N_2O is 0.40–1.01‰. The total contribution from microbial nitrification and denitrification, biomass burning, industrial processes, NH_2+ NO_2, and N + NO_2 is 0.46‰ [*Kaiser and Röckmann*, 2005]. These results suggest that either mechanism B is invalid or there are

undiscovered sinks for $\Delta^{17}O$, if we assume that Kaiser and Röckmann's estimate of 0.46% is applicable. Paleoatmospheric trace gas concentrations preserved in ice cores provide a wealth of information on biogeochemical cycles involving carbon, nitrogen, and oxygen. The $\delta^{15}N$ and $\delta^{18}O$ of N_2O over the past 30,000 years have been measured in ice cores [*Sowers et al.*, 2003]. An extension to $\delta^{17}O$ or $\Delta^{17}O$ will provide additional information. The linear relationship (Figure 4) between the strength of atmospheric N_2O sources and $\Delta^{17}O$ anomaly in N_2O can be used to constrain ozone levels in paleoatmospheres.

[33] **Acknowledgments.** This work was supported in part by NSF grant ATM-9903790 to California Institute of Technology and NSC grant 95-2111-M-001-009 to Academia Sinica. Special thanks is due X. Jiang for the derivation of the WACCM circulation used in two-dimensional modeling and W. DeMore, S. Prasad, and S. Sander on the discussion of the kinetics of N_2O production in the atmosphere. We thank X. Jiang, V. Natraj, N. Heavens, C. Parkinson, and R.-L. Shia for their critical reading of the manuscript.

References

Andrews, D. G., J. R. Holton, and C. B. Leovy (1987), *Middle Atmosphere Dynamics*, Elsevier, New York.

Bhattacharya, S. K., S. Chakraborty, J. Savarino, and M. H. Thiemens (2002), Low-pressure dependency of the isotopic enrichment in ozone: Stratospheric implications, *J. Geophys. Res. Atmos.*, *107*, Art. No. 4675.

Brenninkmeijer, C. A. M., C. Janssen, J. Kaiser, T. Rockmann, T. S. Rhee, and S. S. Assonov (2003), Isotope effects in the chemistry of atmospheric trace compounds, *Chem. Rev.*, *103*, 5125–5161.

Blake, G. A., M. C. Liang, C. G. Morgan, and Y. L. Yung (2003), A Born-Oppenheimer photolysis model of N_2O fractionation, *Geophys. Res. Lett.*, *30*(12), 1656, doi:10.1029/2003GL016932.

Cliff, S. S., and M. H. Thiemens (1997), The $^{18}O/^{16}O$ and $^{17}O/^{16}O$ ratios in atmospheric nitrous oxide: A mass-independent anomaly, *Science*, *278*, 1774–1776.

Cliff, S. S., C. A. M. Brenninkmeijer, and M. H. Thiemens (1999), First measurement of the $^{18}O/^{16}O$ and $^{17}O/^{16}O$ ratios in stratospheric nitrous oxide: A mass-independent anomaly, *J. Geophys. Res. Atmos.*, *104*, 16,171–16,175.

DeMore, W., and O. F. Raper (1962), Reaction of O (^1D) with nitrogen, *J. Chem. Phys.*, *37*, 2048–2052.

Estupiñán, E. G., J. M. Nicovich, J. Li, D. M. Cunnold, and P. H. Wine (2002), Investigation of N_2O production from 266 and 532 nm laser flash photolysis of $O_3/N_2/O_2$ mixtures, *J. Phys. Chem. A*, *106*, 5880–5890.

Gaedtke, H., K. Glanzer, H. Hippler, K. Luther, and J. Troe (1972), Addition reactions of oxygen atoms at high pressures, Fourteenth Symposium (International) on Combustion, 295–303.

Gao, Y. Q., and R. A. Marcus (2001), Strange and unconventional isotope effects in ozone formation, *Science*, *293*, 259–263.

Intergovernmental Panel on Climate Change (IPCC) (2001), Climate Change: The Scientific Basis, edited by J. T. Houghton et al., Cambridge Univ. Press, New York.

Jiang, X., C. D. Camp, R. Shia, D. Noone, C. Walker, and Y. L. Yung (2004), Quasi-biennial oscillation and quasi-biennial oscillation-annual beat in the tropical total column ozone: A two-dimensional model simulation, *J. Geophys. Res. Atmos.*, *109*.

Johnson, M. S., G. Billing, A. Gruodis, and M. Janssen (2001), Photolysis of nitrous oxide isotopomers studied by time-dependent hermite propagation, *J. Phys. Chem. A*, *105*, 8672–8680.

Johnston, J. C., and M. H. Thiemens (1997), The isotopic composition of tropospheric ozone in three environments, *J. Geophys. Res. Atmos.*, *102*, 25,395–25,404.

Kim, K. R., and H. Craig (1993), ^{15}N and ^{18}O Characteristics of nitrous oxide—A global perspective, *Science*, *262*, 1855–1857.

Kaiser, J., T. Röckmann, and C. A. M. Brenninkmeijer (2004), Contribution of mass-dependent fractionation to the oxygen isotope anomaly of atmospheric nitrous oxide, *J. Geophys. Res. Atmos.*, *109*.

Kaiser, J., and T. Röckmann (2005), Absence of isotope exchange in the reaction of $N_2O + O$ (^1D) and the global $\Delta^{17}O$ budget of nitrous oxide, *Geophys. Res. Lett.*, *32*, L15808, doi:10.1029/2005GL023199.

Kajimoto, O., and R. J. Cvetanovic (1976), Formation of nitrous-oxide in reaction of O ($^1D_2$) atoms with nitrogen, *J. Chem. Phys.*, *64*, 1005–1015.

Krankowsky, D., P. Lämmerzahl, and K. Mauersberger (2000), Isotopic measurements of stratospheric ozone, *Geophys. Res. Lett.*, *27*, 2593–2595.

Lämmerzahl, P., T. Röckmann, C. A. M. Brenninkmeijer, D. Krankowsky, and K. Mauersberger (2002), Oxygen isotope composition of stratospheric carbon dioxide, *Geophys. Res. Lett.*, *29*(12), 1582, doi:10.1029/2001GL014343.

Liang, M. C., G. A. Blake, B. R. Lewis, and Y. L. Yung (2007), Oxygen isotopic composition of carbon dioxide in the middle atmosphere, Proceedings of the National Academy of Sciences of the United States of America, 104, 21–25.

Liang, M. C., G. A. Blake, and Y. L. Yung (2004), A semianalytic model for photo-induced isotopic fractionation in simple molecules, *J. Geophys. Res. Atmos.*, *109*(D10), art. no. D10308.

Liang, M. C., F. W. Irion, J. D. Weibel, C. E. Miller, G. A. Blake, and Y. L. Yung (2006), Isotopic composition of stratospheric ozone, *J. Geophys. Res. Atmos.*, *111*.

Maric, D., and J. P. Burrows (1992), Formation of N_2O in the photolysis photoexcitation of NO, NO_2 and air, *J. Photochem. Photobiol. A, Chem.*, *66*, 291–312.

Mauersberger, K. (1987), Ozone isotope measurements in the stratosphere, *Geophys. Res. Lett.*, *14*, 80–83.

Mauersberger, K., B. Erbacher, D. Krankowsky, J. Gunther, and R. Nickel (1999), Ozone isotope enrichment: Isotopomer-specific rate coefficients, *Science*, *283*, 370–372.

Mauersberger, K., P. Lämmerzahl, and D. Krankowsky (2001), Stratospheric ozone isotope enrichments-revisited, *Geophys. Res. Lett.*, *28*, 3155–3158.

McElroy, M. B., and D. B. A. Jones (1996), Evidence for an additional source of atmospheric N_2O, *Global Biogeochem. Cycles*, *10*, 651–659.

McLinden, C. A., M. J. Prather, and M. S. Johnson (2003), Global modeling of the isotopic analogues of N_2O: Stratospheric distributions, budgets, and the ^{17}O-^{18}O mass-independent anomaly, *J. Geophys. Res. Atmos.*, *108*, art. no. 4233.

Michalski, G., Z. Scott, M. Kabiling, and M. H. Thiemens (2003), First measurements and modeling of $\Delta^{17}O$ in atmospheric nitrate, *Geophys. Res. Lett.*, *30*(16), 1870, doi:10.1029/2003GL017015.

Miller, C. E., R. M. Onorato, M. C. Liang, and Y. L. Yung (2005), Extraordinary isotopic fractionation in ozone photolysis, *Geophys. Res. Lett.*, *32*, L14814, doi:10.1029/2005GL023160.

Morgan, C. G., M. Allen, M. C. Liang, R. L. Shia, G. A. Blake, and Y. L. Yung (2004), Isotopic fractionation of nitrous oxide in the stratosphere: Comparison between model and observations, *J. Geophys. Res. Atmos.*, *109*(D4), art. no. D04305.

Prasad, S. S. (2002), A new model of N_2O quantum yield in the UV photolysis of $O_3/O_2/N_2$ mixtures: Contributions of electronically excited O_3 and O_3-N_2, *J. Chem. Phys.*, *117*, 10,104–10,108.

Prakash, M. K., J. D. Weibel, and R. A. Marcus (2005), Isotopomer fractionation in the UV photolysis of N_2O: Comparison of theory and experiment, *J. Geophys. Res. Atmos.*, *110*, art. no. D21315.

Prasad, S. S. (2005), Especially significant new component of N_2O quantum yield in the UV photolysis of O_3 in air, *J. Phys. Chem. A*, *109*, 9035–9043.

Röckmann, T., J. Kaiser, J. N. Crowley, C. A. M. Brenninkmeijer, and P. J. Crutzen (2001), The origin of the anomalous or "mass-independent" oxygen isotope fractionation in tropospheric N_2O, *Geophys. Res. Lett.*, *28*, 503–506.

Sander, S. P., B. J. Finlayson-Pitts, R. R. Friedl, D. M. Golden, R. E. Huie, H. Keller-Rudek, C. E. Kolb, M. J. Kurylo, M. J. Molina, G. K. Moortgat, V. L. Orkin, A. R. Ravishankara, and P. H. Wine (2006), Chemical Kinetics and Photochemical Data for Use in Atmospheric Studies, *Evaluation Number 15, JPL Publication 06-2*, Jet Propulsion Laboratory, Pasadena.

Sassi, F., R. R. Garcia, B. A. Boville, and H. Liu (2002), On temperature inversions and the mesospheric surf zone, *J. Geophys. Res. Atmos.*, *107*.

Sassi, F., D. Kinnison, B. A. Boville, R. R. Garcia, and R. Roble (2004), Effect of El Niño-Southern Oscillation on the dynamical, thermal, and chemical structure of the middle atmosphere, *J. Geophys. Res. Atmos.*, *109*.

Sowers, T., R. B. Alley, and J. Jubenville (2003), Ice core records of atmospheric N_2O covering the last 106,000 years, *Science*, *301*, 945.

Stein, L. Y., and Y. L. Yung (2003), Production, isotopic composition, and atmospheric fate of biologically produced nitrous oxide, *Annu. Rev. Earth Planet. Sci.*, *31*, 329–356.

Summers, M. E., D. E. Siskind, J. T. Bacmeister, R. R. Conway, S. E. Zasadil, and D. F. Strobel (1997), Seasonal variation of middle atmospheric CH_4 and H_2O with a new chemical-dynamical model, *J. Geophys. Res. Atmos.*, *102*, 3503–3526.

Thiemens, M. H. (2006), History and applications of mass-independent isotope effects, *Annu. Rev. Earth Planet. Sci.*, *34*, 217–262.

Thiemens, M. H., and J. E. Heidenreich (1983), The mass-independent fractionation of oxygen—A novel isotope effect and its possible cosmochemical implications, *Science*, *219*, 1073–1075.

Yung, Y. L., M. C. Liang, G. A. Blake, R. P. Muller, and C. E. Miller (2004), Evidence for O-atom exchange in the O (^{1}D)+N_2O reaction as the source of mass-independent isotopic fractionation in atmospheric N_2O, *Geophys. Res. Lett.*, *31*, L19106, doi:10.1029/2004GL020950.

Zellner, R., D. Hartmann, and I. Rosner (1992), N_2O Formation in the reactive collisional quenching of NO_3^* and NO_2^* by N_2, *Ber. Bunsen Ges. Phys. Chem. Chem. Phys.*, *96*, 385–390.

Zipf, E. C., and S. S. Prasad (1998), Experimental evidence that excited ozone is a source of nitrous oxide, *Geophys. Res. Lett.*, *25*, 4333–4336.

M.-C. Liang, Research Center for Environmental Changes, Academia Sinica, Taipei 115, Taiwan. (mcl@rcec.sinica.edu.tw)

Y. L. Yung, Division of Geological and Planetary Sciences, California Institute of Technology, MS150-21, 1200 E. California Blvd., Pasadena, CA 91125, USA. (yly@gps.caltech.edu)